BIOLOGY OF REPRODUCTION (2015) **93**(3):72, 1–17
Published online before print 29 July 2015.
DOI 10.1095/biolreprod.115.131318

Male Rat Germ Cells Display Age-Dependent and Cell-Specific Susceptibility in Response to Oxidative Stress Challenges[1]

Johanna Selvaratnam,[3] Catriona Paul,[3] and Bernard Robaire[2,3,4]

[3]*Department of Pharmacology and Therapeutics, McGill University, Montréal, Québec, Canada*
[4]*Department of Obstetrics and Gynecology, McGill University, Montréal, Québec, Canada*

ABSTRACT

For decades male germ cells were considered unaffected by aging, due to the fact that males continue to generate sperm into old age; however, evidence indicates that germ cells from aged males are of lower quality than those of young males. The current study examines the effects of aging on pachytene spermatocytes and round spermatids, and is the first study to culture these cells in isolation for an extended period. Our objective is to determine the cell-specific responses germ cells have to aging and oxidative insult. Culturing isolated germ cells from young and aged Brown Norway rats revealed that germ cells from aged males displayed an earlier decline in viability, elevated levels of reactive oxygen species (ROS), and increased spermatocyte DNA damage, compared to young males. Furthermore, oxidative insult by prooxidant 3-morpholinosydnonimine provides insight into how spermatocytes and spermatids manage excess ROS. Genome-wide microarray analyses revealed that several transcripts for antioxidants, *Sod1, Cat,* and *Prdxs,* were up-regulated in response to ROS in germ cells from young males while being expressed at lower levels in the aged. In contrast, the expression of DNA damage repair genes *Rad50* and *Atm* were increased in the germ cells from aged animals. Our data indicate that as germ cells undergo spermatogenesis, they adapt and respond to oxidative stress differently, depending on their phase of development, and the process of aging results in redox dysfunction. Thus, even at early stages of spermatogenesis, germ cells from aged males are unable to mount an appropriate response to manage oxidative stress.

aging, gene expression, oxidative stress, spermatid, spermatocyte

INTRODUCTION

Advanced paternal age has been overlooked for decades but is now recognized for the negative impact it has on fertility and progeny. Many studies provide evidence that as men age the quality of their germ cells deteriorates, with increasing levels of DNA damage, resulting in a decline in male fertility [1–5]. By the time a man reaches 38 yr of age, the spermatozoa he produces displays on average three-times greater DNA damage compared to that of a younger man [4]. Increasing concern over paternal age has largely been due to mounting evidence that the damage in germ cells of aged men contributes to diseases in offspring, such as autism [6–8], achondroplasia [9], schizophrenia [10], and attention-deficit/hyperactivity disorder [11].

Paternal aging is associated with abnormal spermatozoal morphology and motility [12, 13], increased oxidative stress [14], reduced antioxidant activity [15], and greater spermatozoal DNA damage [5, 16]. While evidence suggests that spermatozoa from aging males display a reduced capacity to respond to oxidative stress [15, 17], the effects of aging on germ cells, as they progress through spermatogenesis, is not known. Moreover, the responses of aged developing germ cells to oxidative stress remain unclear, and even less is known about germ cell-specific antioxidant mechanisms that play a role in aging throughout the process of spermatogenesis.

Spermatogenesis is a highly dynamic process. Spermatogonia undergo several mitotic divisions prior to entering meiosis, where, as spermatocytes, they undergo two meiotic divisions that result in the formation of haploid round spermatids. Spermatids undergo extensive changes including chromatin condensation and remodeling before being transformed into spermatozoa. Given the continuous and dynamic nature of spermatogenesis, germ cells generate copious amount of free radicals or reactive oxygen species (ROS) as by-products of cellular metabolism [18, 19]. While a certain quantity of ROS is essential for normal cellular functions, such as cell signaling, homeostasis [20], and processes such as capacitation that allows the sperm to fertilize the oocyte [21], a major problem arises when ROS are generated in excess. The accumulation of free radicals can cause extensive damage to macromolecules, including nucleic acids, proteins, and lipids [22]. Under normal conditions, cells have sophisticated antioxidant defense systems [23–25] that work in concert to protect developing germ cells from exposure to excessive ROS; however, with aging the natural balance between ROS and antioxidants is disrupted [17, 25, 26].

Free radicals such as superoxide ($\bullet O_2^-$) and hydroxyl ($\bullet HO$) are generated as by-products of the electron transport chain and neutralized by cellular antioxidant enzymes. Several antioxidant pathways work together to ensure the management of free radicals [25–27]. Cytoplasmic antioxidant superoxide dismutase 1 (SOD1) breaks down $\bullet O_2^-$ into hydrogen peroxide (H_2O_2), which can then be further neutralized by enzymes such as catalase (CAT), peroxiredoxins (PRDXs), glutathione peroxidases (GPXs), and glutathione S-transferases (GSTs) [25].

Previous studies have investigated oxidative stress and aging-associated damage primarily in mature spermatozoa [15, 16] that have undergone compaction and are transcriptionally and translationally inactive. This makes it critical to examine germ cells in earlier phases of spermatogenesis to uncover possible mechanisms responsible for altered germ cell quality during aging. However, there is limited knowledge in this area, with few studies investigating the effects of oxidative stress in

[1]These studies were supported by grant MOP-89767 from CIHR. C.P. is a recipient of a CIHR Postdoctoral Fellowship. B.R. is a James McGill Professor.
[2]Correspondence: Bernard Robaire, Department of Pharmacology & Therapeutics, McGill University, 3655 Promenade Sir-William-Osler, Montréal, Québec, Canada H3G 1Y6.
E-mail: bernard.robaire@mcgill.ca

Received: 5 May 2015.
First decision: 18 June 2015.
Accepted: 27 July 2015.

eISSN: 1529-7268 http://www.biolreprod.org
ISSN: 0006-3363

early germ cells such as spermatocytes or spermatids [28, 29], and fewer still examining germ-cell-specific responses without supporting Sertoli cells. The presence of Sertoli nurse cells, which provide nourishment, developmental factors, a protective barrier, and antioxidants, has masked germ-cell-specific responses to oxidative stress. Consequently, we established a novel model for culturing rat germ cells in isolation, which unlike previous models enables long-term culture of germ cells, without Sertoli cells, allowing for the study of antioxidant defenses specific to each germ cell type.

To test the response of germ cells to oxidative stress, it was essential to expose these isolated and cultured germ cells from both young and aged rats to an oxidative insult. The prooxidant 3-morpholinosydnonimine (SIN-1) is a nitric oxide donor and can cause cytotoxic effects on cells [30]; when administered to cultured cells, it results in the continuous release of radicals: $\bullet O_2^-$, •HO, and peroxynitrite ($ONOO^-$). Thus SIN-1 treatment challenges cells to use their existing antioxidant defenses to respond and protect themselves from oxidative damage. In addition to this prooxidant, an antioxidant EUK-134 (chloro([2,2′-[1,2-ethanediylbis [{nitrilo-κN} methylidyne]]-*bis*[6-methoxyphenolato-κO]])-manganese), hereafter referred to as EUK, was also administered. This salen-manganese complex, is a low-molecular-weight synthetic compound that shows both SOD and CAT activities, catalytically neutralizing $\bullet O_2^-$ and H_2O_2, respectively [31]. EUK was used to investigate how isolated germ cells respond to antioxidant exposure and determine whether antioxidant treatment could prevent/alleviate the negative effects of SIN-1 insult on germ cells.

We hypothesize that germ cells from aged males respond to oxidative stress less effectively and display greater difficulty in removing damaging ROS than those from young males, rendering germ cells from older males more susceptible to DNA damage. Furthermore, this model will provide a clearer understanding of aging-related germ cell-specific alterations in antioxidant status and the mechanisms activated in response to oxidative stress.

MATERIALS AND METHODS

Animals

Male Brown Norway rats of 4 and 18 mo of age (6 animals per group) were maintained on a 12L:12D cycle; food and water were provided ad libitum. Young rats (4-mo-old) were purchased directly from Harlan (Indianapolis, IN), while aged rats were purchased from Harlan via the National Institute of Aging (Bethesda, MD). Eighteen months of age is the time point just prior to the onset of germ cell loss and testicular atrophy [28, 29]. All animal handling and care was done in accordance with the guidelines established by the Canadian Council of Animal Care (McGill Animal Resources Centre Protocol # 4687).

Cell Isolation and Separation

Each rat was checked for the presence of regressed testes (<1.4g); only those rats that did not have regressed testes were used in this study. Spermatogenic cells were obtained through cell separation using the STA-PUT velocity sedimentation technique as described by Bellvé et al. [32] and modified by Aguilar-Mahecha et al. [28]. Briefly, the tunica albuginea was removed along with any large blood vessels; the parenchyma was subjected to enzymatic digestion at 34°C first with 0.5 mg/ml collagenase (Sigma Aldrich Canada, Oakville, ON, Canada) for 12 min in continuous agitation (120 cycles/min). This was followed by sedimentation and washing with 0.5 mg/ml trypsin (Type I, T8003; Sigma, St. Louis, MO) and DNase I (Type I, DN-25; Sigma) for 16 min. After dissociation, cells were filtered through a nylon mesh (70 μm) and washed with RPMI (RPMI medium 160; Invitrogen, Burlington, ON, Canada) containing 0.5% bovine serum albumin (BSA). Cells were centrifuged and filtered (50 μm), and 5.6×10^8 cells in 25 ml of 0.5% BSA/RPMI were loaded into the velocity sedimentation apparatus (STA-PUT; Proscience, Don Mills, ON, Canada) and separated on a 2%–4% BSA gradient in RPMI by sedimentation at unit gravity. Fractions of pachytene spermatocytes and round spermatids were identified by phase contrast microscopy. Fractions with an average purity of > 85% (not less than 83%) were pooled.

TABLE 1. List of treatment groups.

Treatment groups*	Treatment details	Treatment descriptions
T0	0 h Control (media only)	Cells analyzed after isolation
T13	13 h Control (media only)	Cells analyzed at beginning of treatment
T17	17 h Control (media only)	Cells analyzed at end of treatment
SIN-1	17 h 1 mM SIN-1 (4 h)	Cells treated with prooxidant
EUK	17 h 10 mM EUK (30 min) Media only (4 h)	Cells pretreated with antioxidant
SIN-1+EUK	17 h 10 mM EUK (30 min) 1 mM SIN-1 (4 h)	Cells pretreated with antioxidant and then treated with prooxidant

* SIN-1, 3-morpholinosydnonimine; EUK, chloro([2,2′-[1,2-ethanediylbis [{nitrilo-κN} methylidyne]]*bis*[6-methoxyphenolato-κO]])-manganese.

Long-Term Culture of Isolated Germ Cells

Isolated pachytene spermatocytes, round spermatids, and elongated spermatids were seeded onto 96-well culture plates (250 000 cells/well) in 5% CO_2 at 32°C, in phenol-red-free media supplemented with 5% fetal bovine serum (Sigma Aldrich) adapted from La Salle et al. [33]. Cultured cells were photographed at various time points from 0 to 48 h following isolation (T0–T48). Following each time point, aliquots of cells were collected, pelleted, and stored at −80°C until use.

Prooxidant and Antioxidant Drug Treatments

Isolated germ cells were treated with the following drugs: SIN-1 (Sigma Aldrich Canada) and EUK (Cayman Chemicals, Ann Arbor, MI). Isolated germ cells were treated with either media-only (controls) or 1 mM SIN-1 for 4 h with additional treatment groups pretreated 30 min prior to prooxidant treatment with 10 mM EUK (Table 1 and Supplemental Fig. S1; Supplemental Data are available online at www.biolreprod.org). Following each treatment, an aliquot of cells were collected, pelleted, and stored at −80°C until use.

The drug concentrations were chosen according to previous studies [34–36] and preliminary dose-response trials that indicated that a minimum of 1 mM of SIN-1 was required to induce a ROS response without obvious signs of toxicity in cultured germ cells; 1 mM SIN1-1 was previously used [34] and shown to induce minimal lethality in cell lines [35, 36]. EUK-134 concentration of 10 mM was chosen to pretreat several groups of cultured germ cells because this dose was previously shown to both alleviate ROS in vitro [37] and increase longevity in vivo [38]. The window of treatment was chosen based on the unaltered viability from T13–T17 in all cultured primary cells from both young and aged rats.

Viability Assessment

Isolated and cultured pachytene spermatocytes and round spermatids were assessed for viability using trypan blue exclusion from T0, when the cells were plated to T48 (48 h from plating), and following treatments.

High Content Screening: Cellular ROS and Apoptosis Analysis

Following culture and treatment, aliquots of isolated cells were incubated in the nuclear stain Hoechst (2,5′-bi-1H-benzimidazole, 2′-[4-ethoxyphenyl]-5-[4-methyl-1-piperazinyl]; Invitrogen, Burlington, ON) and flurogenic probe CellROX DeepRed Reagent (Invitrogen) for 30 min at 32°C; following incubation, cells were washed in media and CellEvent Caspase-3/7 Detection Reagent (which detects activated caspase-3 and caspase-7) was added, and the cells were transferred to a 96-well Cell Carrier (PerkinElmer, Woodbridge, ON)

plate with an optically clear bottom. The plate was centrifuged at 1200 rpm at 4°C for 5 min and immediately scanned by the Operetta HTS imaging system (PerkinElmer, Woodbridge, ON, Canada) at 40× magnification with 11 fields of view/well. Image analysis was done with Columbus 2.2 software (PerkinElmer) where mean per well data were calculated, and the software was used to analyze and quantify both cytoplasmic ROS and nuclear caspase3/7 (for apoptosis) in both isolated cell types.

Meiotic Spreads

At the end of each time point and for each treatment, pachytene spermatocytes were dropped using a pipette onto glass slides from a height of ~20 cm. Two drops of 0.05% Triton X-100 (in distilled H_2O) were added to each slide for 10 min at room temperature followed by eight drops of fixative (2% formaldehyde, 0.02% SDS, pH 8.0) per slide and incubated for 1 h in a humidified chamber. The slides were dipped briefly six times in distilled-H_2O and allowed to air dry for 5 min before storing at −20°C until use.

Spermatocyte DNA-Damage Detection: Meiotic Spread Immunofluorescence

Following DNA double-strand breaks (DSBs), histone H2AX becomes phosphorylated at serine 139 forming γ-H2AX foci that then prompt cellular responses for DNA repair [39]. γ-H2AX has been well characterized in male germ cells [39, 40] and visualized in meiotic spread where they appear normally in the sex-body of pachytene spermatocytes (see Fig. 7A). To visualize and be able to quantify γ-H2AX foci on chromosome spreads, we used an antibody to detect synaptonemal complex protein 3, (SYCP3), a component of mammalian meiotic chromosome cores [41, 42].

The slides were defrosted by washing in PBS for 5 min and blocked with blocking buffer (5% goat serum, 0.5% BSA, and 0.1% Tween-20) for 1 h at room temperature. The primary antibodies anti-SYCP3 mouse monoclonal (1:400; Abcam, Cambridge, MA) and anti-gamma H2AX (an active component of the DNA damage response [43]) rabbit polyclonal (1:200; Upstate Biotechnology, Charlottesville, VA) were diluted in blocking buffer and incubated overnight in a humidified chamber at 36°C. After three 5-min washes in PBS, the secondary antibodies (goat anti-mouse Alexa-546 and goat anti-rabbit Alexa-488, both 1:200; Molecular Probes, Invitrogen) were applied and incubated for 1 h at room temperature. Following three further washes in PBS, slides were incubated with 4′,6-diamidino-2-phenylindole nuclear stain (Sigma) at 1:1000 in PBS for 10 min before two final PBS washes. Finally, the slides were mounted in Vectashield mounting medium (Vector Laboratories, Burlington, ON). Images were taken using a multiphoton Leica TCS SP8 MP microscope. Blind counts of the number of foci falling on the synaptonemal complexes were done for at least 50 pachytene spermatocytes from each rat.

RNA Extraction and Microarray

Total RNA was extracted from the pachytene spermatocyte and round spermatid fractions (~1×10^6 cells) using TRIzol (Invitrogen), and RNA was cleaned-up using RNeasy kit columns (Qiagen, Mississauga, ON, Canada). The RNA concentration was determined using a Nanodrop 2000 (Nanodrop Technologies, Wilmington, DE) and quality assessed using a Bioanalyzer 2100 Expert (Agilent Technologies, Santa Clara, CA). Gene expression analysis was done using Agilent SurePrint G3 Rat GE 8x60K Microarray Kit. RNA (50 ng) was reverse transcribed, and the cRNA was labeled and then hybridized onto the microarray according to the manufacturer's instructions (Agilent Technologies: One-Color Microarray-Based Gene Expression Analysis Protocol). The raw data obtained were quantile shift normalized (Genespring v11.0, Agilent Technologies). All data were placed in GEO (Accession No. GSE66976, National Center for Biotechnology Information). Statistical significance between the groups was tested by two-way-ANOVA using a P-value of < 0.05 and the Benjamini-Hochburg post hoc test. Probe sets that were significantly altered were further filtered using a minimum 2-fold difference.

Real-Time Quantitative Reverse Transcriptase-PCR

RNA was diluted to a working concentration of 2 ng/μl, and RT-PCR was done using Power SYBR Green RNA-to-C_T 1-Step Kit according to the manufacturer's instructions on OneStepPlus Real-Time PCR System (Applied Biosystems). PCR thermal cycling parameters were: 40°C for 30 min and 95°C for 5 min (one cycle), 95°C for 15 sec, and 60°C for 30 sec (40 cycles). Standard curves were generated using 0.1, 1, 10, and 100 ng/ml of RNA from a control young mixed-germ cell sample in each run for quantification. RT-PCR primers (Table 2) were ready-made Quantitect Primers (Qiagen) and those for Rn18s were designed using Primer3 software (http://frodo.wi.mit.edu) and provided by Alpha DNA (Montreal, QC; forward primer 5′-CCTCCAATG GATCCTCGTTA-3′; reverse primer 5′-AAACGGCTACCACATCCAAG-3′). The expression levels of all genes of interest were corrected using an endogenous control, 18S rRNA; the relative ratio of mRNA expression of the samples was determined. The results shown are the means from four rats per group with each standard and sample being analyzed in duplicate.

Statistical Analyses

Results are expressed as means and standard errors of the mean. The statistical tests used were: two-way ANOVA with Bonferroni multiple comparison test (see Figs. 1, 10, and 11), one-way ANOVA with Bonferroni multiple comparisons test (see Fig. 2), Student t-test (see Figs. 3–6), Kruskal-Wallis with Dunn multiple comparisons test (see Figs. 7 and 8), two-way ANOVA with Benjamini-Hochberg correction and Bonferroni multiple comparison test (see Fig. 9). All analyses were done using GraphPad Prism version 5 (Graph Pad Software Inc., San Diego, CA).

RESULTS

Decreased Survival of Aged Germ Cells in Long-Term Culture

When first isolated, spermatocytes appeared spherical with fairly large nuclei that contained dense aggregates. As they progressed through time in culture, projections extended from the spermatocytes, and the cells became more sickle in shape from T4–T21, with dying cells and debris detected from T24–T48 (Fig. 1A). Isolated spermatocytes from either young or aged males display no significant difference in viability from T0–T17. By T21 the viability of spermatocytes from aged rats began to decline, and from T24–T48 their viability dropped steeply to below 50%, while viability of spermatocytes from young rats remained significantly higher at T24–48 (Fig. 1B).

Round spermatids appeared perfectly spherical with well-defined nuclei. As they progressed through time in culture, the nucleus moved from a centered to an apical position in the cells, and very small projections were observed from T8–T24 (Fig. 1C). Isolated round spermatids displayed no age-related decline in viability until T21, and a steady decline was further observed in spermatids from aged rats compared to those from young rats (Fig. 1D). Isolated elongated spermatids showed a rapid decline in their viability by T4, which continued to drop to levels below 70%, and 50% by T13 in elongating spermatids from young and aged rats, respectively (Supplemental Fig. S2). Due to their low viability, the culture of elongated spermatids was discontinued.

Prooxidant SIN-1 Significantly Decrease the Viability of Spermatids of Aged Animals

The sites of action of SIN-1 and EUK are shown in Figure 2A. Administration of 1 mM SIN-1 induced similar significant decreases in viability of pachytene spermatocyte from young and aged animals (Fig. 2B). EUK-only treatment showed no effect, while the SIN-1 treatment effect was completely prevented by pretreatment with EUK (Fig. 2B).

SIN-1 administration induced a significant decrease in the viability of round spermatids from both young and aged animals. Round spermatids from aged animals displayed a significantly lower viability following SIN-1 treatment when compared to that of young animals (Fig. 2C).

Elevated ROS in Isolated and Cultured Germ Cells of Aged Animals

At both T13 and T17, pachytene spermatocytes from aged animals show significant increases in ROS when compared to those from young animals (Fig. 3A), with representative live-

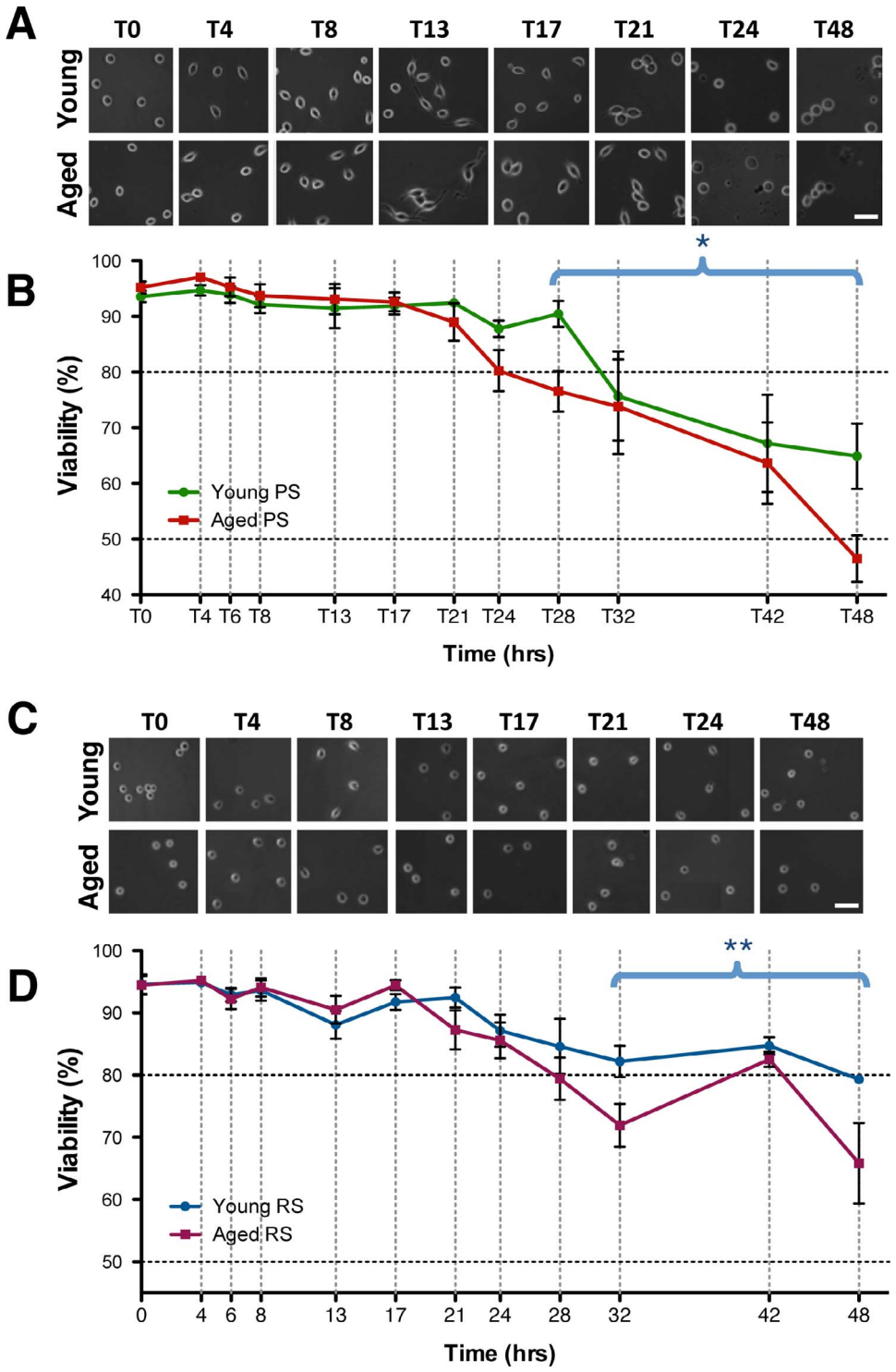

FIG. 1. The viability of isolated male germ cells with increasing time in culture. Morphology of cells through time in culture is shown with phase-contrast images of spermatocytes (**A**) and spermatids (**C**) in culture. Bar = 25 μm. The viability of cultured isolated spermatocytes (**B**) and round spermatids (**D**) from young and aged animals are plotted from 0 to 48 h. Error bars represent the SEM (n = 5–8); two-way ANOVA, Bonferroni post hoc test, $*P < 0.05$; $**P < 0.005$.

cell images displaying the cytoplasmic ROS (red) quantified (Fig. 3C). Similarly, round spermatids from aged animals display increased ROS in culture at T13 and T17 when compared to those from young animals (Fig. 3, B and D).

Pachytene spermatocytes of young animals generate ROS above control levels following SIN-1 and SIN-1+EUK treatment, while with EUK-only, ROS levels remain at control levels. Spermatocytes from aged animals show ROS levels constantly higher than control levels (Fig. 4; orange dotted line—untreated cells collected at T17). Age-related effects were observed with EUK-only pretreatment, showing that spermatocytes from young rats respond to EUK pretreatment

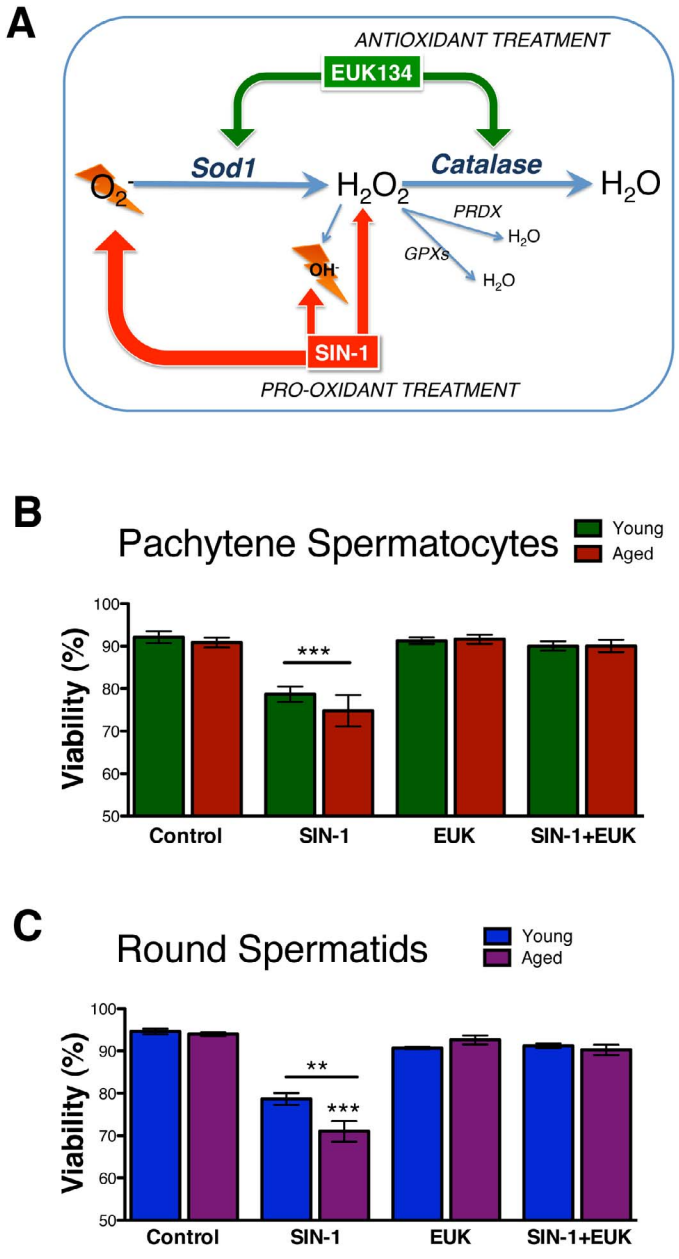

FIG. 2. The viability of isolated and cultured germ cells following in vitro prooxidant and antioxidant treatments. A schematic displays the mechanisms of action by prooxidant SIN-1 and antioxidant EUK (**A**). The control viabilities from T0–T17 show no changes (data not shown); T17 values are shown as controls. SIN-1 reduces viability in both spermatocytes (**B**) and spermatids (**C**) versus controls. Error bars represent the SEM (n = 5–8); one-way ANOVA with Bonferroni multiple comparisons test; n = 6; $^{**}P < 0.001$; $^{***}P < 0.0001$.

with control levels of ROS while EUK does not decrease the high ROS levels measured in spermatocytes from aged rats (Fig. 4, A and C).

Round spermatids from young and aged animals show ROS levels falling below control levels following SIN-1 treatment, with age-related effects observed with EUK-only treatment in which spermatids from young animals show control-level ROS while EUK does not affect the high levels of ROS measured in aged animal spermatids. Increased ROS, above control levels, is detected with the SIN-1+EUK treatment in spermatids from both young and aged animals (Fig. 4, B and D). EUK may reduce/down-regulate the natural cellular antioxidants in round spermatids, thus leaving the round spermatids from aged animals unable to reduce ROS following exposure to EUK.

Increased Apoptosis in Isolated and Cultured Germ Cells from Aged Animals

Apoptosis levels were determined by measuring the mean intensity of activated nuclear caspase3/7 per cell. Analyses of both mean caspase3/7 nuclear intensity per cell per sample (Fig. 5), and the percentage of apoptotic cells with nuclear intensity above a set threshold (Supplemental Fig. S3), were determined. Staurosporine treated positive control samples displayed significantly high levels of apoptosis versus T13 and T17 (Fig. 5, A and B, and Supplemental Fig. S3, A and C).

With increasing time in culture from T13 to T17, there were no significant differences between levels of apoptosis in spermatocytes (Fig. 5, A and C) and in spermatids (Fig. 5, B and D). While the percentage of apoptotic cells was unaltered from T13 to T17, a significantly higher percentage of apoptotic spermatocytes were detected in aged versus young animals (Supplemental Fig. S3A). SIN-1 treatment did not have any significant effects on apoptosis levels in spermatocytes or spermatids from either young or aged animals (Fig, 6). However, further analyses of the results support out earlier viability data (Fig. 2C) with spermatids from aged rats showing a significantly increased percentage of apoptotic cells (Supplemental Fig. S3A) following SIN-1 treatment. Moreover, the combined stress of age and SIN-1 treatment is most evident in the percentage of apoptotic spermatids from aged animals.

Increased DNA Damage in Spermatocytes of Aged Animals

At T0, spermatocytes from both young and aged animals show no significant difference in DNA damage. With increasing time in culture, spermatocytes from young animals show a trend of gradual increase in mean γ-H2AX foci per spermatocyte from T13 to T24, and this trend plateaus from T24 to T48 (Fig. 7, A and B). In aged animals, spermatocytes show a dramatic increase in mean γ-H2AX foci per spermatocyte with prolonged time in culture from T13 to T48 (Fig. 7, A and B). Age effects are observed, with spermatocytes showing significantly increased foci at T13 and T48 in aged animals versus young.

SIN-1 Significantly Increases DNA Damage in Spermatocyte of Aged Animals

A significant age effect was observed with increased γ-H2AX foci in the control (T17) samples of the aged animals versus the young (Fig. 8). SIN-1 treatment increased the mean γ-H2AX foci per spermatocyte in young animals by 5.8-fold compared to controls from young animals, and in aged animals by 5.5-fold compared to controls from aged animals. Furthermore a significant age effect was observed with spermatocytes from aged animals showing 1.4-fold increase in γ-H2AX foci following SIN-1 treatment versus their counterparts from young animals (Fig. 8). EUK-only-treated spermatocytes of both young and aged rats displayed control levels of γ-H2AX foci, while SIN-1+EUK treatment showed that pretreatment with EUK inhibited the SIN-1 induced formation of high numbers of γ-H2AX foci in both young and aged animals.

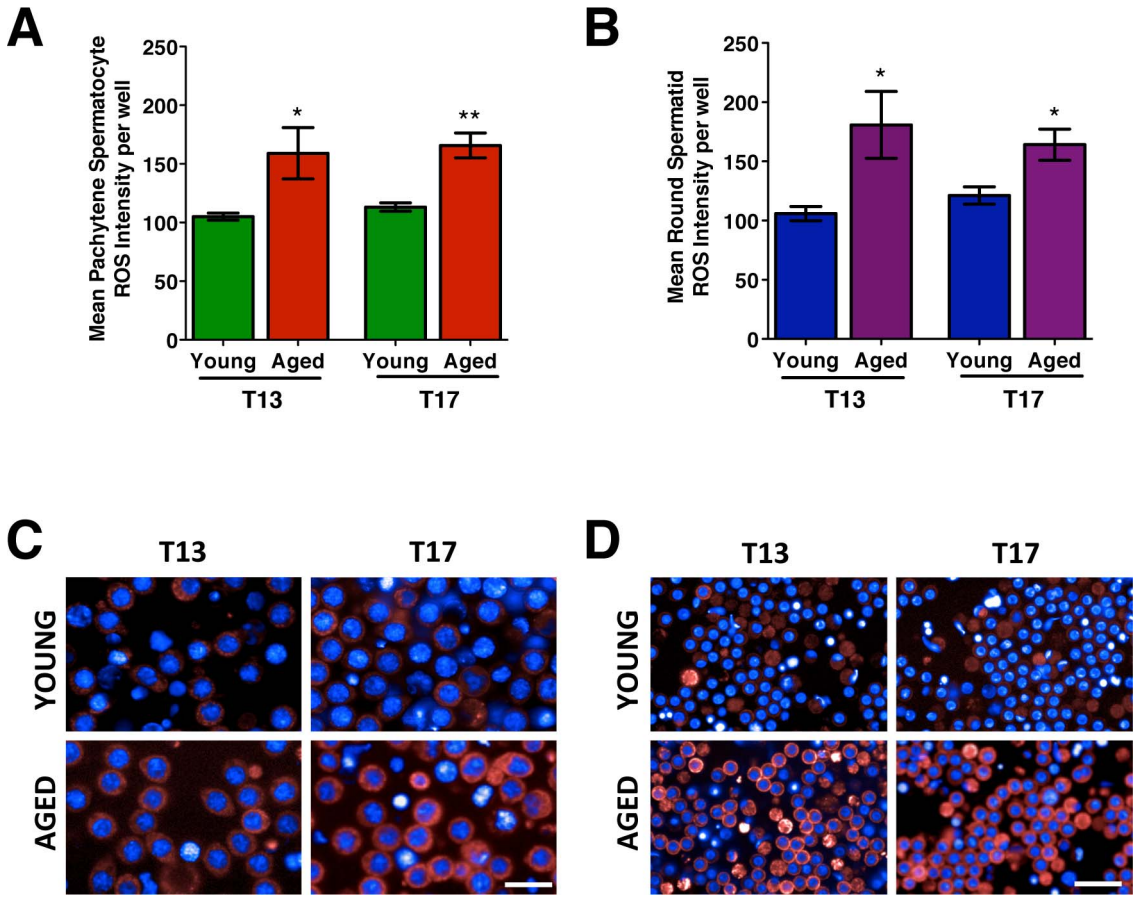

FIG. 3. The mean ROS intensity measured in isolated and cultured male germ cells. The mean ROS intensity measured at T13 and T17 in spermatocytes (**A**) and spermatids (**B**), with representative images of spermatocytes (**C**) and spermatids (**D**) from young and aged animals. The images show ROS detected with CellROX DeepRed Reagent as a red cytoplasmic fluorescence and nuclei visualized using Hoechst (blue). Error bars represent the SEM; Student *t*-test; n = 4–6; $*P < 0.05$, $**P < 0.01$. Bar = 25 μm.

Genome-Wide Analysis Identifies Cell-Specific Regulation of Antioxidants and DNA-Damage Responses to Oxidative Stress and Aging

We assessed the impact of SIN-1 and EUK treatments on isolated and cultured germ cells from young and aged animals by examining genome-wide changes in transcript expression. Principle component analysis (PCA) was used to reduce the dimensionality of the gene expression data sets (n = 4–5) and make easier discernment between the general relationships of groups (Fig. 9). A mixed germ cell (MGC) fraction consisting of cells collected prior to germ cell separation was used as a control sample loaded on each microarray slide to account for slide to slide variation. From the PCA, it was clear that the spermatocytes, round spermatids, and MGC controls had distinct gene-expression signatures and occupied different spaces within the PCA plot (Fig. 9A). Further analysis between spermatocytes from young and aged animals also showed distinct gene expression signatures between the two groups (Fig. 9B), and similar distinct spaces within the PCA plot were observed for round spermatids from young and aged animals (Fig. 9C).

Microarray analyses indicated that 2123 transcripts were significantly changed by at least 2-fold in spermatocytes during aging (Fig. 10A), with 245 transcripts being exclusively altered in spermatocytes of young rats, while 122 were altered in spermatocytes of aged rats (Fig. 10A). In spermatids, 1930 transcripts were altered in response to aging (Fig. 10B), with 52 being expressed exclusively in spermatids from young animals and 130 in spermatids of aged rats (Fig. 10B). The genes were clustered into groups to identify which transcripts were exclusively expressed in each treatment group for spermatocytes (Fig. 10, C and D) and spermatids (Fig. 10, E and F). Further analyses of these > 2-fold significantly altered transcripts indicated that 59 transcripts were exclusively detected in the control group of spermatocytes of young animals, while 48 transcripts were detected in spermatocytes from aged animals (Fig. 10, C and D). In spermatids, 218 transcripts were exclusively detected in the control group from young animals, and 58 transcripts were detected in the control groups of aged animals (Fig. 10, E and F). In response to SIN-1 treatment in spermatocytes, four transcripts were exclusively detected in young animals, while 237 transcripts were detected in aged animals. Spermatids in contrast expressed 124 transcripts in response to SIN-1 treatment in young animals and 264 transcripts in aged animals (for a complete list of genes see Supplemental Table S1). EUK treatment induced 161 transcripts exclusively in spermatocytes of young animals and 77 transcripts in aged animals, while spermatids treated with EUK expressed 18 transcripts exclusively in young animals, and 63 transcripts in aged animals. Finally, the combined SIN-1+EUK treatment induced 156 transcripts in spermatocytes from young animals and 18 in aged animal spermatocytes, with

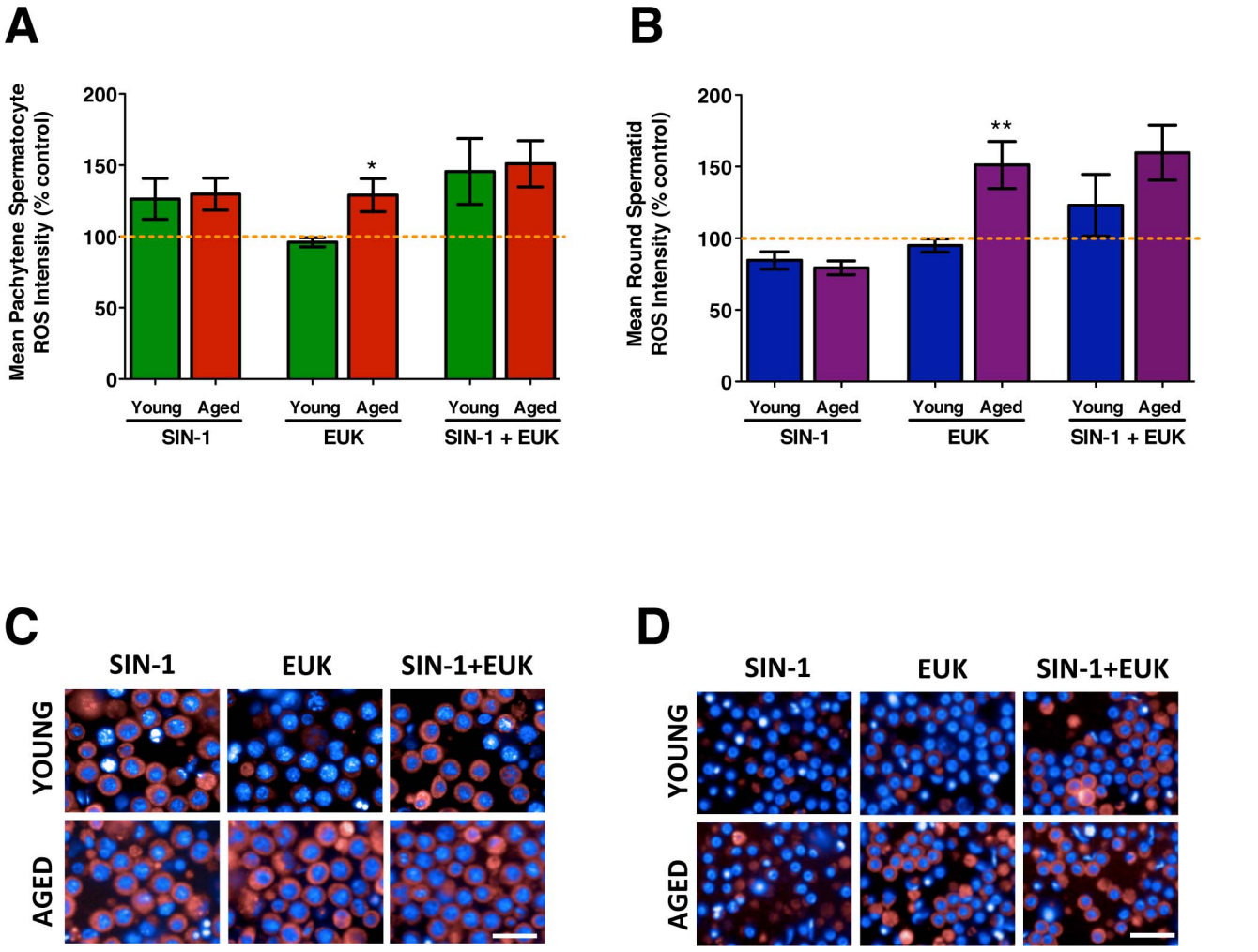

FIG. 4. The mean ROS intensity measured in isolated and cultured male germ cells following in vitro treatments. Mean ROS intensity measured in spermatocytes (**A**) and spermatids (**B**) from young and aged animals treated with SIN-1, EUK, and SIN-1+EUK. The orange dotted line represents control levels of ROS from untreated cells T17 (end time for all treatments). The representative images display spermatocytes (**C**) and spermatids (**D**) from young and aged animals with CellROX DeepRed Reagent indicating cytoplasmic ROS (red) and nuclei visualized with Hoechst (blue). Error bars represent the SEM; Student *t*-test; n = 4–6; $*P < 0.05$, $**P < 0.01$. Bar = 25 μm.

spermatids expressing 105 and 96 transcripts in young and aged animals, respectively.

Analyses of the microarray yielded groups of both antioxidants and DNA repair molecules that were significantly altered between groups our treatment groups, we chose to validate the expression of those genes that displayed significant > 2-fold differences. The microarray results were validated using quantitative reverse transcriptase-PCR (qRT-PCR) (Table 2). While the antioxidants *Cat* and *Prdx3* and *6* were highly expressed in pachytene spermatocytes, higher expression of *Sod1* and *Prdx4* was detected in round spermatids (Fig. 11). Age had significant effects on the expression of antioxidants, with lower expression of *Sod1, Cat, and Prdx3 and 4* observed in the spermatocytes from aged animals versus young. SIN-1 treatment maintained this observed age effect, and in the case of certain antioxidants further decreased antioxidant expression (*Sod1, Prdx4*) in the spermatocytes from aged animals. EUK treatment did not alleviate the drop in antioxidants observed in spermatocytes from aged animals; however, minor effects of EUK treatment were noticed with *Cat* and *Prdx3*. The expression of which was increased in both EUK and SIN-1+EUK treated groups of spermatocytes from aged animals (Fig. 11, C and E).

In round spermatids, the antioxidants *Sod1* and *Prdx3, 4,* and *6* showed a trend to be higher in aged animals compared to young ones (Fig. 11. B, F, H, and J). SIN-1 treatment of round spermatids uniformly resulted in decreased *Cat* in young and aged animals, and this drop was not observed with EUK pretreatment, which kept expression of *Cat* at control levels, while the SIN-1+EUK treatment prevented the SIN-1-induced drop in *Cat* expression (Fig. 11D). In response to SIN-1 treatment, *Sod1* is decreased in spermatids of young animals, while it remains at high levels in aged animals (Fig. 11B). EUK treatment causes increased expression of *Sod1,* while SIN-1+EUK treatments result in *Sod1* at control levels of expression, thus indicating EUK treatment prevents SIN-1 induced drop in *Sod1* in spermatids of young animals (Fig. 11B).

In addition to antioxidant transcripts, several DNA-damage response components were significantly altered in expression with both age and treatment. In aged animals, pachytene spermatocytes showed a trend to have higher *Rad50* expression. *Rad50,* a structural maintenance protein and essential for

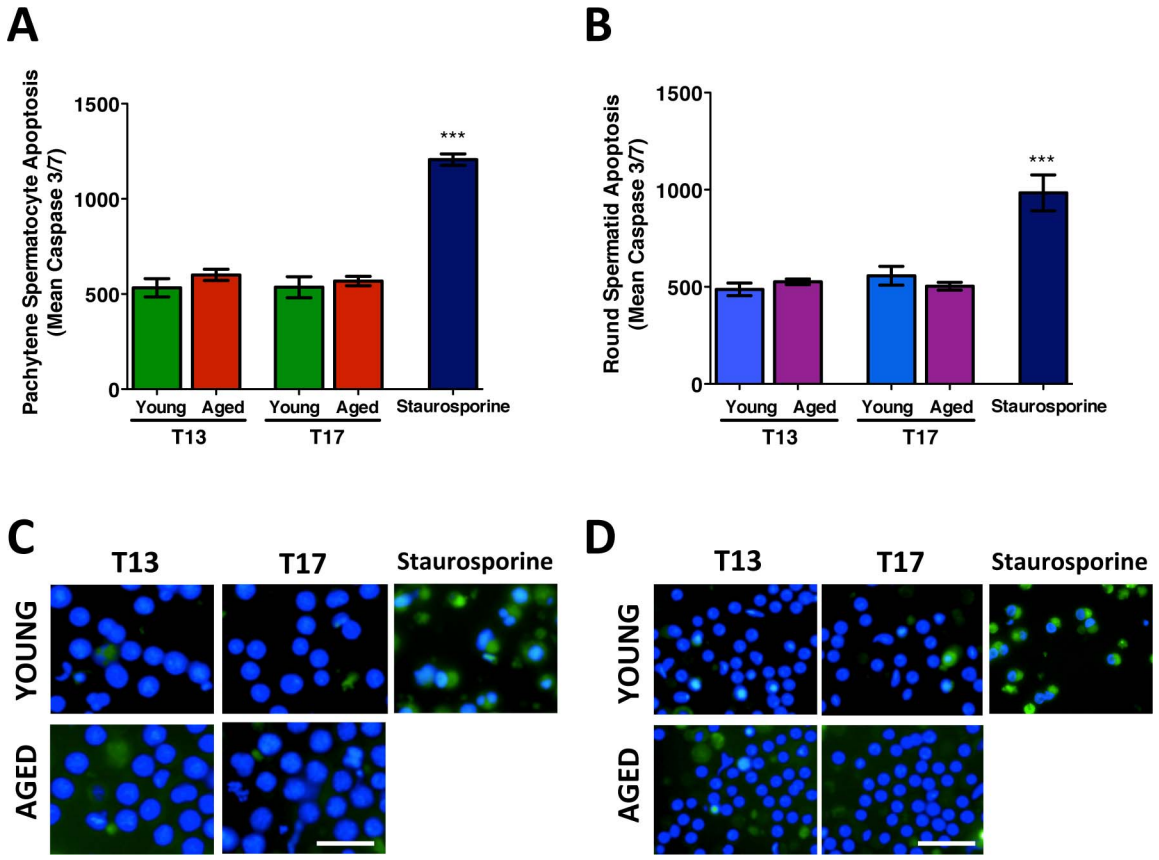

FIG. 5. The mean apoptotic signal measured in isolated male germ cells with increasing time in culture. The mean apoptotic nuclear intensity (indicative of activated caspase 3 and caspase 7) in spermatocytes (**A**) and spermatids (**B**) from young and aged animals at T13 and T17, with staurosporine treated cells as a positive control for nuclear apoptotic intensity. The corresponding images show spermatocytes (**C**) and spermatids (**D**) with probe CellEvent Caspase 3/7 appearing as a nuclear fluorescent signal and nuclei visualized using Hoechst (blue). Error bars represent the SEM; Student *t*-test; n = 4–6; ***$P < 0.0001$. Bar = 25 μm.

the repair of DSBs [44], was significantly increased only in spermatocytes of aged animals with SIN-1 treatment, and the expression of *Rad50* was also high in EUK treated and SIN-1+EUK treated spermatocytes of aged animals (Fig. 12A). In addition, Ataxia-telangiectasia mutated (*Atm*), a DNA damage sensor that activates signaling upon detection of DSBs/apoptosis/genotoxic stress [45, 46], was highly up-regulated in spermatocytes from aged animals. SIN-1 administration causes down-regulation of *Atm* in spermatocytes of aged animals, but EUK and SIN-1+EUK show no significant age-related effects on *Atm* expression (Fig. 12C). 8-Oxoguanine DNA glycosylase (*Ogg1*), a DNA repair enzyme responsible for the excision of mutagenic bases by-product (8-oxoguanine) that is a result of exposure to ROS [47], was significantly lower in expression in SIN-1 treated spermatocytes of young animals than in those of aged ones. EUK treatment reduced *Ogg1* expression in spermatocytes of both young and aged animals (Fig. 12G).

In round spermatids *Rad50* and *Atm* were only dramatically up-regulated in the SIN-1 treated spermatids of aged animals (Fig. 12, B and D), with EUK and SIN-1+EUK treatments reducing this expression to near control levels. SIN-1 treatment down-regulates *Ogg1* expression in spermatids from young animals (Fig. 12H). A particular DNA-repair component highly expressed in round spermatids is apurinic/apyrimidinic endodeoxyribonuclease (*Apex1*), which encodes a protein that plays a key role in repairing single-strand breaks in response to ROS [48]. While spermatids from aged animals show a trend to have higher *Apex1* than those of young animals, with SIN-1 treatment, Apex1 is increased in spermatids from aged animals and decreased in spermatids of young animals, resulting in a highly significant age effect (Fig. 12F). Furthermore, X-ray repair complementing defective repair in Chinese hamster cells 1 (*Xrcc1*) encodes a protein involved in repair of DNA strand breaks [49]; with SIN-1 treatment, it is highly increased in round spermatids from aged, but not young animals (Fig. 12J).

DISCUSSION

Aging reproductive tissues display lower levels of antioxidants [15, 50, 51] and higher levels of ROS [15]; this imbalance contributes to increased cellular damage and other detrimental effects observed with aging. Previous studies have identified the susceptibility of spermatozoa to oxidative stress [52] and the altered DNA repair in pachytene spermatocytes [29] of aged animals; however, the distinct mechanisms that spermatocytes and spermatids use to respond to oxidative stress had previously not been investigated.

The present study analyzed young (4 mo) and aged (18 mo) isolated rat spermatocytes and spermatids, and found that germ cells isolated from young animals survived in culture for longer periods than those from aged animals, while elongated spermatids displayed very poor viability in culture (Supplemental Fig. S2). In aged animals, spermatocytes and round

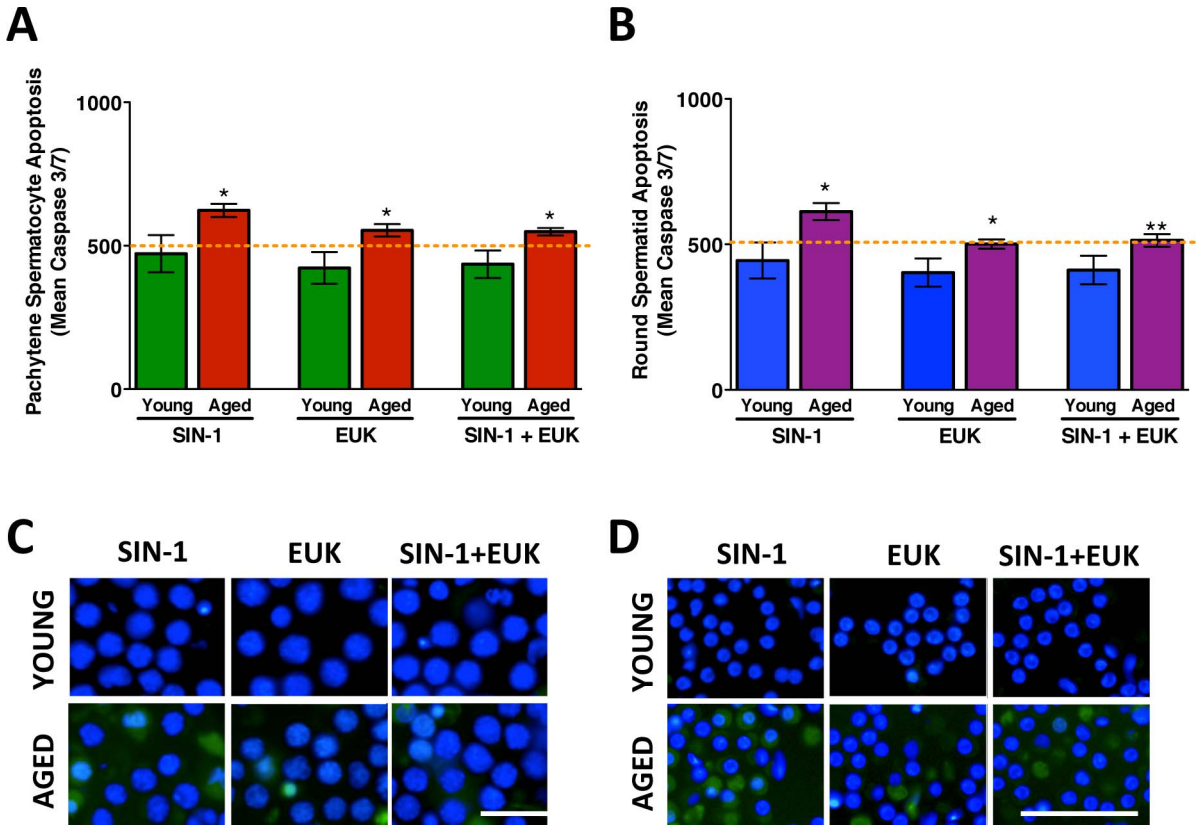

FIG. 6. The mean apoptotic signal measured in isolated and cultured male germ cells following prooxidant and antioxidant treatment. The mean apoptotic nuclear intensity is shown in spermatocytes (**A**) and spermatids (**B**) from young and aged animals following treatment with SIN-1, EUK, and SIN-1+EUK. The orange dotted line represents control levels of apoptotic signal intensity measured from untreated cells T17 (end time for all treatments). The corresponding images show spermatocytes (**C**) and spermatids (**D**) with probe CellEvent Caspase 3/7 appearing as a nuclear fluorescent signal and nuclei visualized using Hoechst (blue). Error bars represent the SEM; Student *t*-tests; n = 6; $*P < 0.05$, $**P < 0.01$. Bar = 25 μm.

spermatids showed higher levels of ROS, with increased DNA damage in spermatocytes (Fig. 7). Validation of genome-wide antioxidants and DNA-repair components, following treatment of these isolated and cultured germ cells with prooxidant SIN-1 and antioxidant EUK, identified the round spermatids of aged animals as less capable of managing redox status following oxidative insult (Figs. 11 and 12).

While this newly established long-term culture of isolated spermatids and spermatocytes are useful models, both the strengths and limitations of this method should be considered. In this culture system, nonadherent germ cells are cultured, free-floating, without the aid of supporting cells/gel-matrix, which adds physical strain on the cells (normally supported by Sertoli cells in vivo). However, the culture of these germ cells in the absence of supporting cells was critical to understand germ cell-specific responses to oxidative stress that can be masked by other cells. Moreover, the culture of primary cells differs significantly from that of immortalized cell lines, as cultured primary cells do not have to adapt to the transformation vectors for immortalization and display greater variation from animal to animal, as seen with our viability data (Figs. 1 and 2).

Additional strain on the cells cultured in this study can be attributed to high oxygen tension. It should be noted that while most cells are cultured under ambient oxygen tension (21%), it has been suggested that the physiological oxygen tension for cells in vivo may be as low as 2%–10% [53]. This commonly used oxygen tension can be an additional oxidative stressor and even cause cells to undergo premature aging [53–55]. Although all of our cells were exposed to the same oxygen tension, it is possible that aged cells may be further affected by oxidative stress generated by high oxygen tension.

Since spermatocytes are transcriptionally active cells, we expected a robust response from these cells towards oxidative stress, while round spermatids were expected to display a minimal response to oxidative insult because they are further along the trajectory to differentiating into more specialized spermatozoa. In addition, previous studies showed round spermatids had relatively few oxidative stress-related transcripts altered as a consequence of aging [29]. However, in the current study where isolated round spermatids were cultured, we identified a clear response of these germ cells to oxidative insult. Given that antioxidants work together in concert to neutralize ROS, the effect of SIN-1 induced oxidative stress on the expression of major antioxidant *Sod1* and the downstream antioxidant *Cat* had to be examined together. SIN-1 treatment had a clear effect decreasing *Cat* expression in round spermatids regardless of the age of the animals, with this decrease being prevented with EUK (Fig. 11D). Previous observations in bovine liver homogenate have reported SIN-1 induced reduction of CAT enzymatic activity in a concentration-dependent manner [56]. Moreover, cytotoxicity studies show that SIN-1 induced endothelial cell death was reduced following administration of CAT [57].

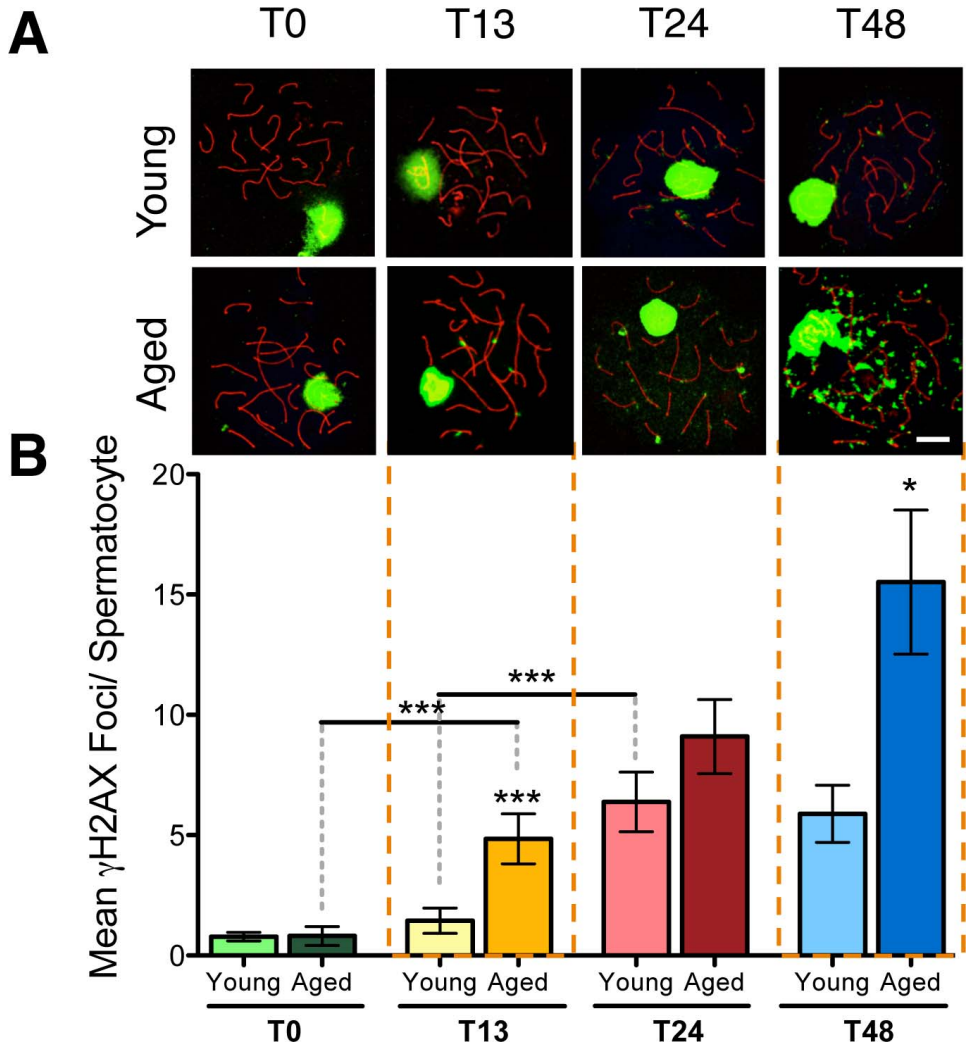

FIG. 7. DNA damage in isolated spermatocytes through time in culture. Meiotic spreads from young and aged animals showing γ-H2AX foci (green) on the synaptonemal complex marked with SYCP3 (red) in pachytene spermatocytes from T0 to T48 (**A**). Kruskal-Wallis with Dunn's multiple comparisons test (**B**); n = 6; *$P < 0.05$, ***$P < 0.0001$. Bar = 10 μm.

Taken together, these data suggest that round spermatids from young animals respond to oxidative insult via regulation of *Sod1* and *Cat,* but that in aged animals, these cells are unable to mount the same response. More specifically, in round spermatids SIN-1 treatment results in the down-regulation of *Cat* and decrease in CAT activity responsible for mopping-up H_2O_2 generated by SOD1 activity. Spermatids of young animals respond to SIN-1 stress by reducing *Sod1*, and the

TABLE 2. List of primers.

Gene	Accession no. or sequence	Quantitect primer no. or sequence
Sod1	NM_017050	QT00174888
Catalase	NM_012520	QT00182700
Prdx2	NM_017169	QT00181496
Prdx3	NM_022540	QT00179375
Prdx4	NM_053512	QT00186123
Prdx6	NM_053576	QT01745765
ATM	NM_001106821	QT01605072
Ogg1	NM_030870	QT00186641
Rad50	NM_022246	QT00191058
Apex1	NM_024148	QT00183281
Xrcc1	NM_053435	QT00186081
Rn18S	S: CCTCCAATGGATCCTCGTTA*	AS: AAACGGCTACCACATCCAAG*

* S, sense; AS, antisense.

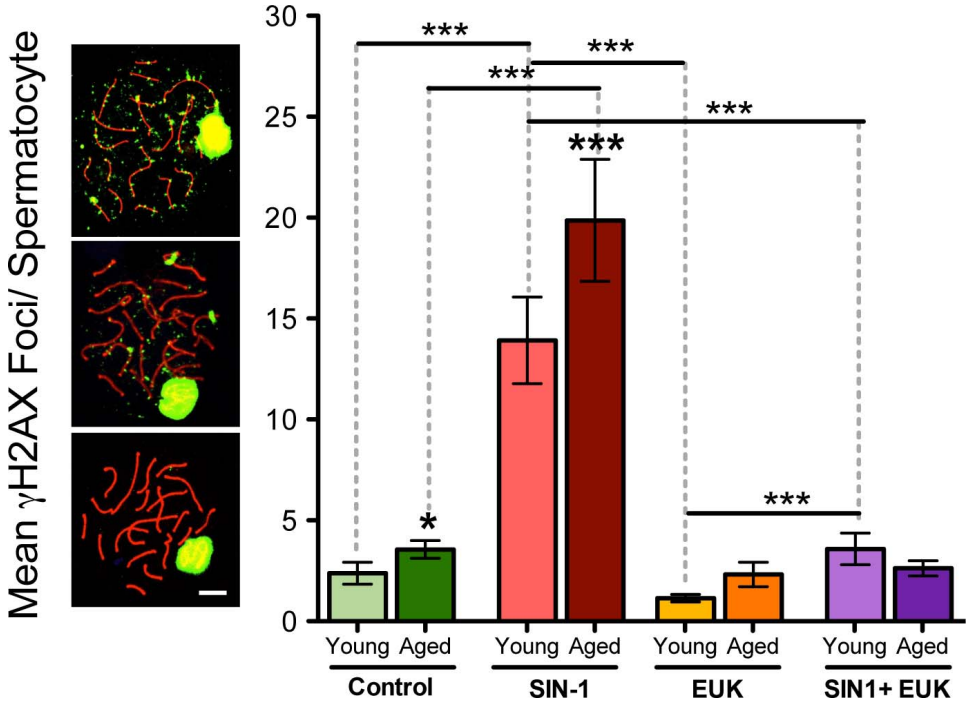

FIG. 8. DNA-damage in isolated spermatocytes after prooxidant and antioxidant treatment. Representative images of foci next to y-axis display γ-H2AX foci in spermatocytes. Graphs shows mean γ-H2AX foci per spermatocyte from young and aged animals following SIN-1, EUK, and SIN-1+EUK treatments. Kruskal-Wallis with Dunn multiple comparisons test; n = 6; $*P < 0.05$, $***P < 0.0001$. Bar = 10 μm.

generation of H_2O_2 in the cell, to cope with the SIN-1 induced reduction of *Cat*. In contrast, spermatids of aged animals continue to express high levels of *Sod1*, resulting in a combination of high *Sod1* and low *Cat*. This suggests excessive H_2O_2, increased ROS-induced damage, and redox imbalance in the spermatids of aged animals. These conclusions are supported by studies of ATM-null mice, in which a decrease in CAT and elevated SOD2 led to progressive deterioration of the redox balance [58]. However, like all biological systems, there are compensatory mechanisms that come into effect; in this case our data suggests *Prdxs* could be compensating for the reduced *Cat*.

Several *Prdxs* were significantly altered with *Prdx3, Prdx4,* and *Prdx6* being increased in SIN-1 treated spermatids of aged animals when compared to young animals. These elevated *Prdxs* may reflect a compensatory mechanism in response to the SIN-1 induced down-regulation of *Cat*, and subsequent redox imbalance. The high expression of *Prdx4* in round spermatids when compared to that of spermatocytes can be attributed to its role in acrosome formation [59]; however, there is speculation that certain isoforms of *Prdx4* in sperm play a role in antioxidant defenses [60]. The most compelling evidence for the critical antioxidant role of these *Prdxs* is revealed through their null mutation mouse models. *Prdx3*$^{-/-}$ and *Prdx6*$^{-/-}$ have increased susceptibility to oxidative stress, and most *Prdx4*$^{-/-}$ have severely reduced testis weight, testis atrophy, and as a result, sterility [61].

While our previous studies have shown altered regulation of DNA repair in spermatocytes of aged rats [29], this is the first study to show evidence of altered DNA repair in spermatids of aged rats in response to stress. This evidence provides additional support to indicate that a redox dysfunction is observed in round spermatids of aged animals that show increased expression of *Rad50* and *Atm* following SIN-1 treatment. Considering that *Atm* is activated by oxidative stress and in the presence of DSBs [45, 62], the complex interplay of antioxidants and DNA repair pathways suggests that as aging disrupts one pathway it will inevitably affect the other. *Atm*-null mice suffer from increased oxidative damage mediated by nitric oxide (NO) [58], as NO readily reacts with $\bullet O_2^-$ resulting in the formation of a highly toxic oxidant $ONOO^-$ [63]. The high expression of *Atm* observed in SIN-1 treated spermatids from aging animals suggests that the generation of $ONOO^-$ within these spermatids could be contributing to the decrease in viability (Fig. 2) and stimulating the increase of *Prdxs*.

Additional repair components *Xrcc1* and *Apex1,* involved in the non-homologous end-joining pathway and repair of DNA damage associated with oxidative stress [64], respectively, are up-regulated in SIN-1 treated spermatids from aged animals, but remain low in young animals. *Xrcc1* is involved in DNA-repair in mouse round spermatids [49]; our data suggest that this is a major mechanism by which spermatids may respond to oxidative stress. Spermatids are known to repair slowly in comparison to other germ cells [49], and the non-homologous end-joining pathway is an error prone process [47]. Therefore the repair of damage is often incomplete, and, since the process of apoptosis is not activated to eliminate these damaged germ cells, the resulting damage can be transmitted to the next generation.

Complementing these results is *Ogg1*, a DNA glycosylase that excises the most frequent mutagenic oxidative base lesion, which shows decreased expression in spermatids from young animals while it remains high in aged animals. These results corroborate previous studies [29] and suggest that increased and excessive DNA damage in spermatids of aged animals results in a greater demand for repair in aged versus young in spermatids.

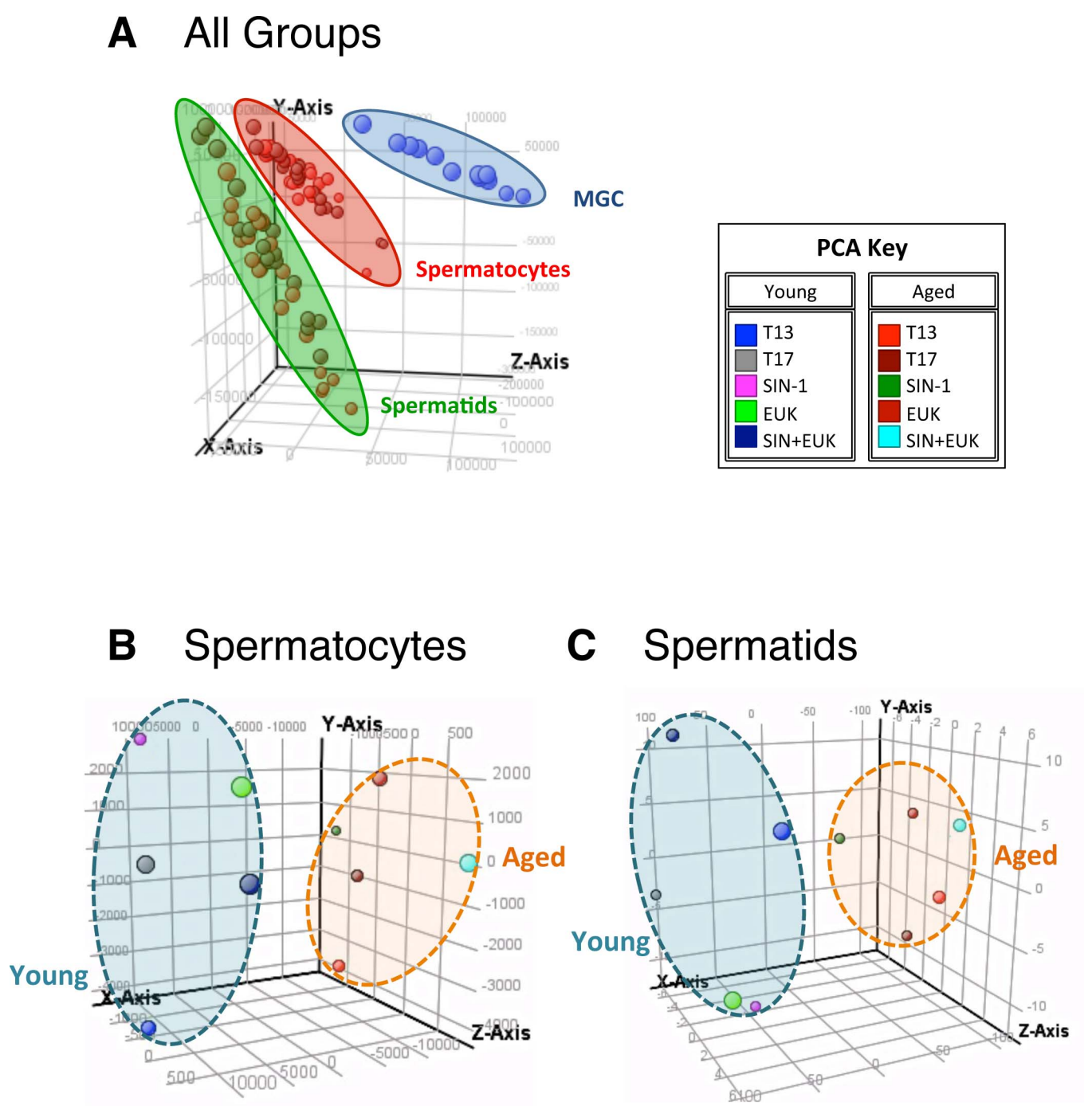

FIG. 9. Principle component analysis (PCA) showing the distribution of samples on a three-dimensional plot. All groups of samples show clear distinctions with mixed germ cell (MGC) controls, spermatocytes, and spermatids clustering together (**A**). Spermatocytes plot (**B**) shows that young and aged animal's spermatocytes occupy distinct spaces, and spermatids (**C**) also show young and aged animals in distinct clusters. PCA key indicated colors of the various treatment groups.

These data suggest that spermatids from aged animals do not cope with oxidative stress as effectively as spermatocytes from young animals. The compounded effects of age with administered oxidative stress exacerbate the limited antioxidant response of spermatids. These finding have also made clear that certain antioxidants are highly expressed in round spermatids, thus indicating that early germ cells without the support of Sertoli cells can mount cell-specific responses to oxidative stress.

In conclusion, our results demonstrate that increased oxidative stress, defined as increased ROS and decreased antioxidant defenses, are observed in isolated and cultured pachytene spermatocytes and round spermatids of aged animals. Furthermore, we show that these cells can mount their own response to an administered oxidative insult in culture, both in terms of antioxidant production and DNA damage repair activation. The method of isolated germ cell culture we have established in this study has also allowed us

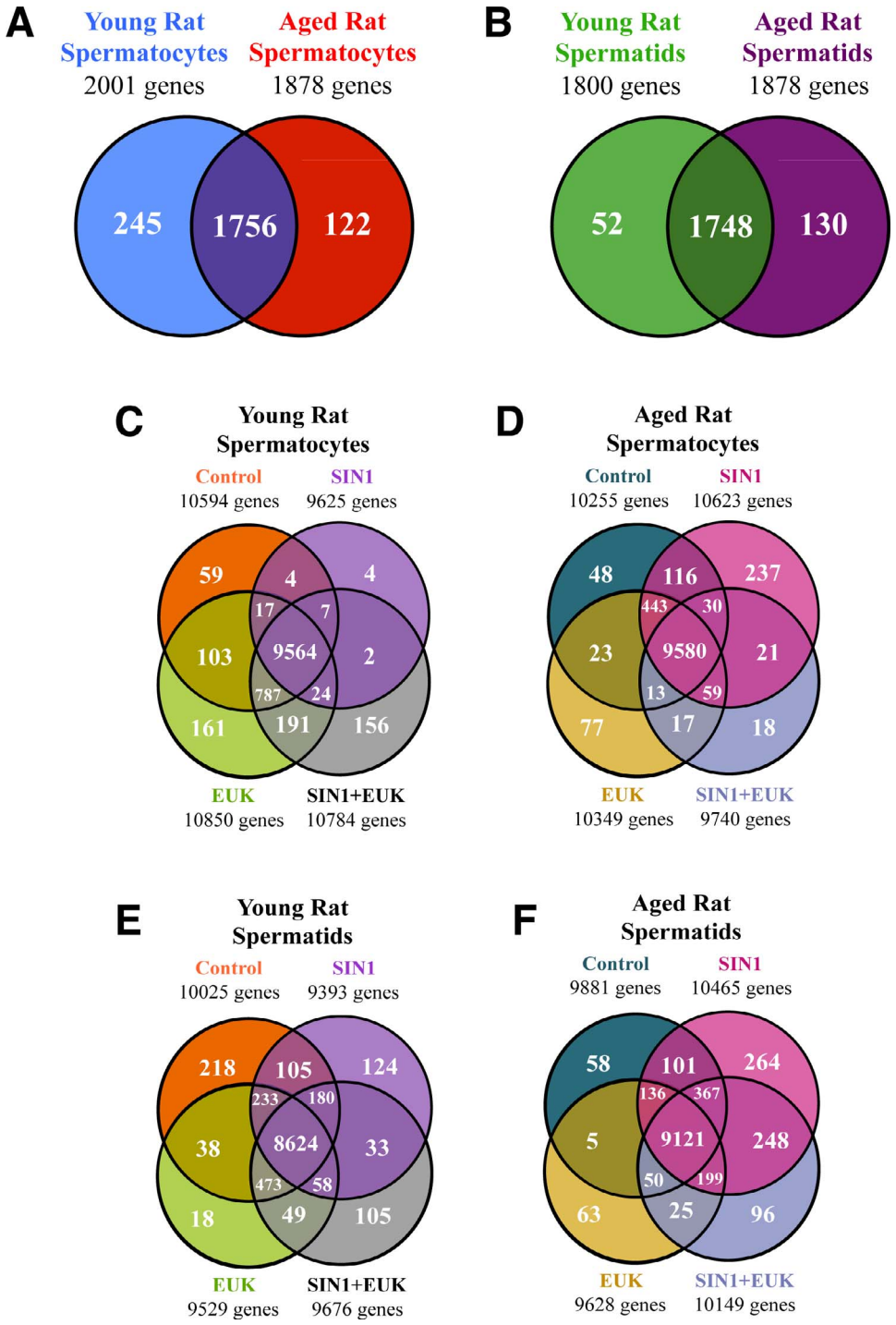

FIG. 10. Genome-wide analyses of isolated and cultured germ cells. Gene expression was examined, and genes with $P < 0.05$ and $\geq$ 2-fold change detected in each experimental group were displayed in Venn diagrams. The numbers of genes significantly altered in spermatocytes (**A**) and spermatids (**B**) from young versus aged animals. The effects of various treatments—control, SIN1, EUK, and SIN1+EUK—on the number of genes significantly altered $\geq$ 2-fold in spermatocytes (**C**) and spermatids (**E**) of young animals and spermatocytes (**D**) and spermatids (**F**) of aged animals. Two-way-ANOVA with Benjamini-Hochberg correction; n = 4–6 per treatment group.

to determine that spermatids from aged animals display a dysfunctional redox response when compared to those of young animals. We have provided evidence that as germ cells of aged animals undergo spermatogenesis they display a progressive loss in their ability to mount the same antioxidant defense mechanisms than those in their young counterparts. Although these studies have begun to provide new insight into how spermatogenic cells respond to the effects of aging and oxidative stress challenge, further studies are required to decipher the complex mechanisms that allow ROS to be eliminated and DNA damage to be repaired in both pachytene spermatocytes and round spermatids. Shedding light on the underlying mechanisms of how aging deteriorates germ cell quality, and leads to redox dysfunction, can provide greater insight into preventative and therapeutic approaches to maintain germ cell quality.

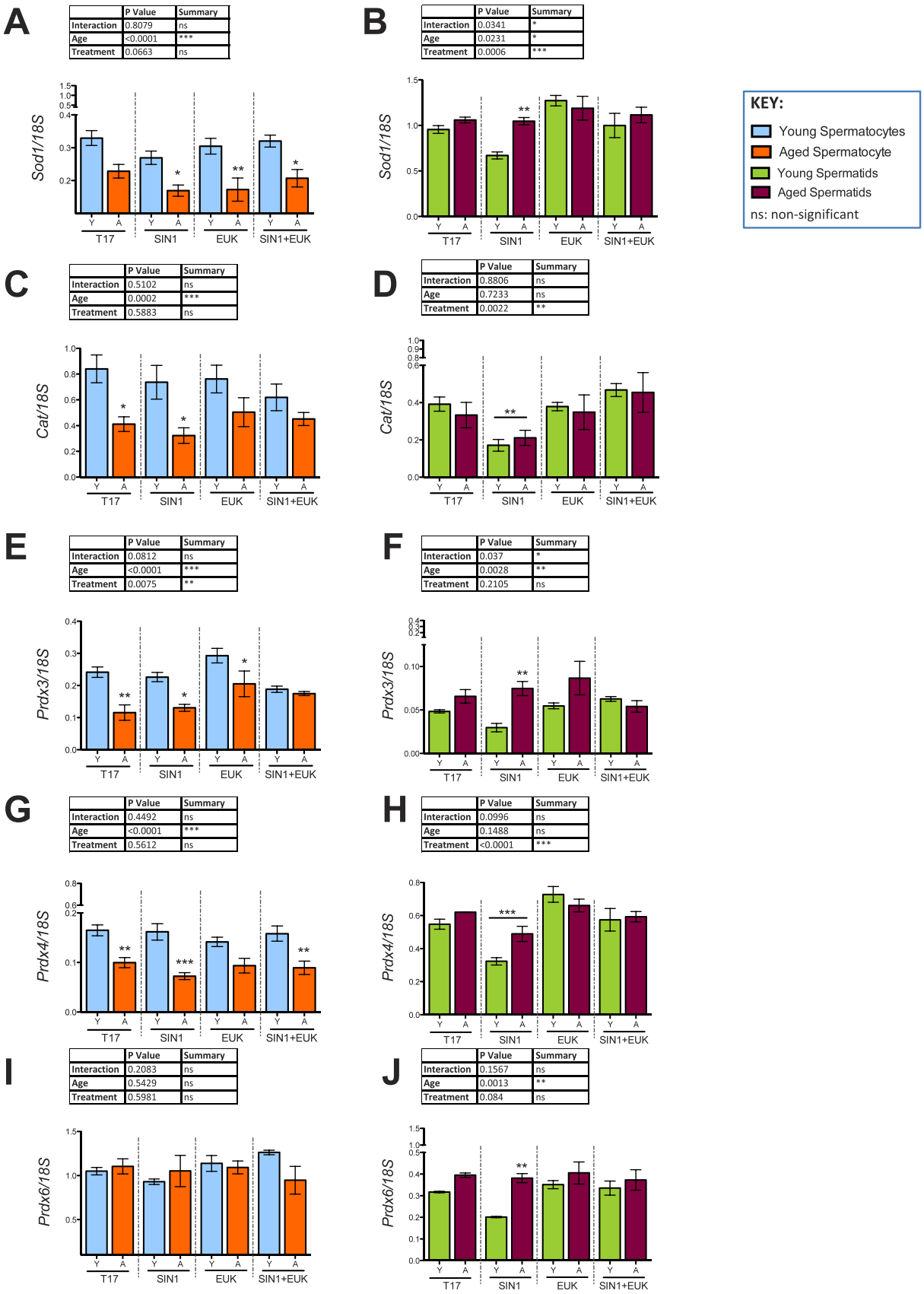

FIG. 11. Validation of antioxidant response in spermatocytes (**A**, **C**, **E**, **G**, **I**) and spermatids (**B**, **D**, **F**, **H**, **J**) from young and aged animals following in vitro prooxidant and antioxidant treatment. Histograms representing gene expression of antioxidants: *Sod1* (**A**, **B**), *Cat* (**C**, **D**), *Prdx3* (**E**, **F**), *Prdx4* (**G**, **H**), and *Prdx6* (**I**, **J**) using qRT-PCR; 18S was used as an internal control in qRT-PCR quantification. Two-way-ANOVA with Bonferroni multiple comparisons test were used; n = 4; $*P < 0.05$, $**P < 0.01$, $***P < 0.0001$.

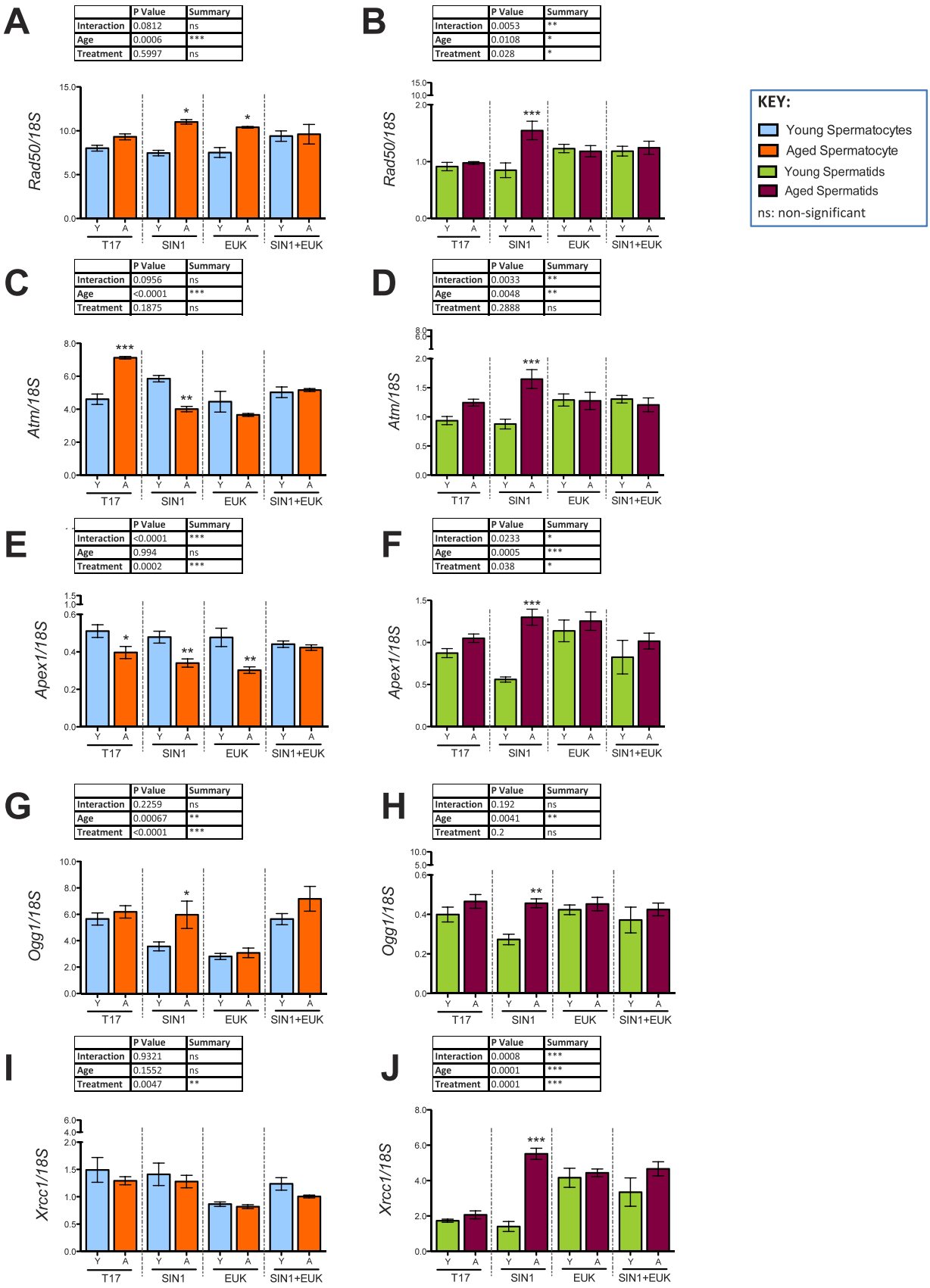

FIG. 12. Validation of DNA-damage repair response in spermatocytes (**A**, **C**, **E**, **G**, **I**) and spermatids (**B**, **D**, **F**, **H**, **J**) from young and aged animals following in vitro prooxidant and antioxidant treatment. Histograms representing gene expression of antioxidants: *Rad50* (**A**, **B**), *Atm* (**C**, **D**), *Apex1* (**E**, **F**), *Ogg1* (**G**, **H**), and *Xrcc1* (**I**, **J**) using qRT-PCR; 18S was used as an internal control in qRT-PCR quantification. Two-way-ANOVA with Bonferroni multiple comparisons test were used; n = 4; $*P < 0.05$, $**P < 0.01$, $***P < 0.0001$.

ACKNOWLEDGMENT

The authors wish to thank Trang Luu for her technical assistance, Dr. Wolfgang Reintsch for his help with imaging and HCS analyses, and Yaned Gaitan for help with microarray hybridization and scanning.

REFERENCES

1. Crosnoe LE, Kim ED. Impact of age on male fertility. Curr Opin Obstet Gynecol 2013; 25:181–185.
2. Kovac JR, Addai J, Smith RP, Coward RM, Lamb DJ, Lipshultz LI. The effects of advanced paternal age on fertility. Asian J Androl 2013; 15: 723–728.
3. Callaway E. Fathers bequeath more mutations as they age. Nature 2012; 488:439.
4. Singh NP, Muller CH, Berger RE. Effects of age on DNA double-strand breaks and apoptosis in human sperm. Fertil Steril 2003; 80:1420–1430.
5. Wyrobek AJ, Eskenazi B, Young S, Arnheim N, Tiemann-Boege I, Jabs EW, Glaser RL, Pearson FS, Evenson D. Advancing age has differential effects on DNA damage, chromatin integrity, gene mutations, and aneuploidies in sperm. Proc Natl Acad Sci U S A 2006; 103:9601–9606.
6. Frans EM, Sandin S, Reichenberg A, Långström N, Lichtenstein P, McGrath JJ, Hultman CM. Autism risk across generations: a population-based study of advancing grandpaternal and paternal age. JAMA Psychiatry 2013; 70:516–521.
7. Hultman CM, Sandin S, Levine SZ, Lichtenstein P, Reichenberg A. Advancing paternal age and risk of autism: new evidence from a population-based study and a meta-analysis of epidemiological studies. Mol Psychiatry 2011; 16:1203–1212.
8. Reichenberg A, Gross R, Weiser M, Bresnahan M, Silverman J, Harlap S, Rabinowitz J, Shulman C, Malaspina D, Lubin G, Knobler HY, Davidson M, et al. Advancing paternal age and autism. Arch Gen Psychiatry 2006; 63:1026–1032.
9. Orioli IM, Castilla EE, Scarano G, Mastroiacovo P. Effect of paternal age in achondroplasia, thanatophoric dysplasia, and osteogenesis imperfecta. Am J Med Genet 1995; 59:209–217.
10. Torrey EF, Buka S, Cannon TD, Goldstein JM, Seidman LJ, Liu T, Hadley T, Rosso IM, Bearden C, Yolken RH. Paternal age as a risk factor for schizophrenia: how important is it? Schizophr Res 2009; 114:1–5.
11. D'Onofrio BM, Rickert ME, Frans E, Kuja-Halkola R, Almqvist C, Sjölander A, Larsson H, Lichtenstein P. Paternal age at childbearing and offspring psychiatric and academic morbidity. JAMA Psychiatry 2014; 71: 432–438.
12. Kidd SA, Eskenazi B, Wyrobek AJ. Effects of male age on semen quality and fertility: a review of the literature. Fertil Steril 2001; 75:237–248.
13. Syntin P, Robaire B. Sperm structural and motility changes during aging in the Brown Norway rat. J Androl 2001; 22:235–244.
14. Smith TB, De Iuliis GN, Lord T, Aitken RJ. The senescence-accelerated mouse prone 8 as a model for oxidative stress and impaired DNA repair in the male germ line. Reproduction 2013; 146:253–262.
15. Weir CP, Robaire B. Spermatozoa have decreased antioxidant enzymatic capacity and increased reactive oxygen species production during aging in the Brown Norway rat. J Androl 2007; 28:229–240.
16. Zubkova EV, Robaire B. Effects of ageing on spermatozoal chromatin and its sensitivity to in vivo and in vitro oxidative challenge in the Brown Norway rat. Hum Reprod 2006; 21:2901–2910.
17. Gershon H, Gershon D. Detection of inactive enzyme molecules in ageing organisms. Nature 1970; 227:1214–1217.
18. Guerriero G, Trocchia S, Abdel-Gawad FK, Ciarcia G. Roles of reactive oxygen species in the spermatogenesis regulation. Front Endocrinol (Lausanne) 2014; 5:56.
19. Fisher HM, Aitken RJ. Comparative analysis of the ability of precursor germ cells and epididymal spermatozoa to generate reactive oxygen metabolites. J Exp Zool 1997; 277:390–400.
20. Ray PD, Huang BW, Tsuji Y. Reactive oxygen species (ROS) homeostasis and redox regulation in cellular signaling. Cell Signal 2012; 24:981–990.
21. O'Flaherty C, Beorlegui N, Beconi MT. Participation of superoxide anion in the capacitation of cryopreserved bovine sperm. Int J Androl 2003; 26: 109–114.
22. Halliwell B, Gutteridge JM. Free radicals, lipid peroxidation, and cell damage. Lancet 1984; 2:1095.
23. O'Flaherty C. The enzymatic antioxidant system of human spermatozoa. Adv Androl 2014; 2014.
24. Bauché F, Fouchard M-H, Jégou B. Antioxidant system in rat testicular cells. FEBS Lett 1994; 349:392–396.
25. Aitken RJ, Roman SD. Antioxidant systems and oxidative stress in the testes. Oxidative Med Cell Longevity 2008; 1:15–24.
26. Luo L, Chen H, Trush MA, Show MD, Anway MD, Zirkin BR. Aging and the brown Norway rat Leydig cell antioxidant defense system. J Androl 2006; 27:240–247.
27. Halliwell B. Free radicals and other reactive species in disease. Wiley Online Library 2005.
28. Aguilar-Mahecha A, Hales BF, Robaire B. Expression of stress response genes in germ cells during spermatogenesis. Biol Reprod 2001; 65: 119–127.
29. Paul C, Nagano M, Robaire B. Aging results in differential regulation of DNA repair pathways in pachytene spermatocytes in the Brown Norway rat. Biol Reprod 2011; 85:1269–1278.
30. Ioannidis I, de Groot H. Cytotoxicity of nitric oxide in Fu5 rat hepatoma cells: evidence for co-operative action with hydrogen peroxide. Biochem J 1993; 296(Pt 2):341–345.
31. Baudry FD. The personal dimension and management of the supervisory situation with a special note on the parallel process. Psychoanal Q 1993; 62:588–614.
32. Bellvé AR, Cavicchia JC, Millette CF, O'Brien DA, Bhatnagar YM, Dym M. Spermatogenic cells of the prepuberal mouse. Isolation and morphological characterization. J Cell Biol 1977; 74:68–85.
33. La Salle S, Sun F, Handel MA. Isolation and short-term culture of mouse spermatocytes for analysis of meiosis. Methods Mol Biol 2009; 558: 279–297.
34. Atorino L, Di Meglio S, Farina B, Jones R, Quesada P. Rat germinal cells require PARP for repair of DNA damage induced by gamma-irradiation and H2O2 treatment. Eur J Cell Biol 2001; 80:222–229.
35. Li CQ, Trudel LJ, Wogan GN. Genotoxicity, mitochondrial damage, and apoptosis in human lymphoblastoid cells exposed to peroxynitrite generated from SIN-1. Chem Res Toxicol 2002; 15:527–535.
36. Doulias PT, Barbouti A, Galaris D, Ischiropoulos H. SIN-1-induced DNA damage in isolated human peripheral blood lymphocytes as assessed by single cell gel electrophoresis (comet assay). Free Radic Biol Med 2001; 30:679–685.
37. Luciani A, Villella VR, Esposito S, Brunetti-Pierri N, Medina D, Settembre C, Gavina M, Pulze L, Giardino I, Pettoello-Mantovani M, D'Apolito M, Guido S, et al. Defective CFTR induces aggresome formation and lung inflammation in cystic fibrosis through ROS-mediated autophagy inhibition. Nat Cell Biol 2010; 12:863–875.
38. Melov S, Ravenscroft J, Malik S, Gill MS, Walker DW, Clayton PE, Wallace DC, Malfroy B, Doctrow SR, Lithgow GJ. Extension of life-span with superoxide dismutase/catalase mimetics. Science 2000; 289: 1567–1569.
39. Hamer G, Roepers-Gajadien HL, van Duyn-Goedhart A, Gademan IS, Kal HB, van Buul PP, de Rooij DG. DNA double-strand breaks and gamma-H2AX signaling in the testis. Biol Reprod 2003; 68:628–634.
40. Fernandez-Capetillo O, Mahadevaiah SK, Celeste A, Romanienko PJ, Camerini-Otero RD, Bonner WM, Manova K, Burgoyne P, Nussenzweig A. H2AX is required for chromatin remodeling and inactivation of sex chromosomes in male mouse meiosis. Dev Cell 2003; 4:497–508.
41. Botelho RJ, DiNicolo L, Tsao N, Karaiskakis A, Tarsounas M, Moens PB, Pearlman RE. The genomic structure of SYCP3, a meiosis-specific gene encoding a protein of the chromosome core. Biochim Biophys Acta 2001; 1518:294–299.
42. Dobson MJ, Pearlman RE, Karaiskakis A, Spyropoulos B, Moens PB. Synaptonemal complex proteins: occurrence, epitope mapping and chromosome disjunction. J Cell Sci 1994; 107(Pt 10):2749–2760.
43. Bassing CH, Chua KF, Sekiguchi J, Suh H, Whitlow SR, Fleming JC, Monroe BC, Ciccone DN, Yan C, Vlasakova K, Livingston DM, Ferguson DO, et al. Increased ionizing radiation sensitivity and genomic instability in the absence of histone H2AX. Proc Natl Acad Sci U S A 2002; 99: 8173–8178.
44. Williams RS, Williams JS, Tainer JA. Mre11-Rad50-Nbs1 is a keystone complex connecting DNA repair machinery, double-strand break signaling, and the chromatin template. Biochem Cell Biol 2007; 85:509–520.
45. Guo Z, Kozlov S, Lavin MF, Person MD, Paull TT. ATM activation by oxidative stress. Science 2010; 330:517–521.
46. Gatei M, Jakob B, Chen P, Kijas AW, Becherel OJ, Gueven N, Birrell G, Lee JH, Paull TT, Lerenthal Y, Fazry S, Taucher-Scholz G, et al. ATM protein-dependent phosphorylation of Rad50 protein regulates DNA repair and cell cycle control. J Biol Chem 2011; 286:31542–31556.
47. Smith TB, Dun MD, Smith ND, Curry BJ, Connaughton HS, Aitken RJ. The presence of a truncated base excision repair pathway in human spermatozoa that is mediated by OGG1. J Cell Sci 2013; 126:1488–1497.
48. Olsen AK, Bjortuft H, Wiger R, Holme J, Seeberg E, Bjoras M, Brunborg G. Highly efficient base excision repair (BER) in human and rat male germ cells. Nucleic Acids Res 2001; 29:1781–1790.
49. Ahmed EA, de Boer P, Philippens ME, Kal HB, de Rooij DG. Parp1-

XRCC1 and the repair of DNA double strand breaks in mouse round spermatids. Mutat Res 2010; 683:84–90.
50. Zubkova EV, Robaire B. Effect of glutathione depletion on antioxidant enzymes in the epididymis, seminal vesicles, and liver and on spermatozoa motility in the aging brown Norway rat. Biol Reprod 2004; 71:1002–1008.
51. Mueller A, Hermo L, Robaire B. The effects of aging on the expression of glutathione S-transferases in the testis and epididymis of the Brown Norway rat. J Androl 1998; 19:450–465.
52. Zubkova EV, Wade M, Robaire B. Changes in spermatozoal chromatin packaging and susceptibility to oxidative challenge during aging. Fertil Steril 2005; 84(Suppl 2):1191–1198.
53. Ho HY, Cheng ML, Cheng PF, Chiu DT. Low oxygen tension alleviates oxidative damage and delays cellular senescence in G6PD-deficient cells. Free Radic Res 2007; 41:571–579.
54. Csete M. Oxygen in the cultivation of stem cells. Ann N Y Acad Sci 2005; 1049:1–8.
55. Wolffe AP, Tata JR. Primary culture, cellular stress and differentiated function. FEBS Lett 1984; 176:8–15.
56. Keng T, Privalle CT, Gilkeson GS, Weinberg JB. Peroxynitrite formation and decreased catalase activity in autoimmune MRL-lpr/lpr mice. Mol Med 2000; 6:779–792.
57. Ishii M, Shimizu S, Momose K, Yamamoto T. SIN-1-induced cytotoxicity in cultured endothelial cells involves reactive oxygen species and nitric oxide: protective effect of sepiapterin. J Cardiovasc Pharmacol 1999; 33: 295–300.
58. Barlow C, Dennery PA, Shigenaga MK, Smith MA, Morrow JD, Roberts LJ II, Wynshaw-Boris A, Levine RL. Loss of the ataxia-telangiectasia gene product causes oxidative damage in target organs. Proc Natl Acad Sci U S A 1999; 96:9915–9919.
59. Sasagawa I, Matsuki S, Suzuki Y, Iuchi Y, Tohya K, Kimura M, Nakada T, Fujii J. Possible involvement of the membrane-bound form of peroxiredoxin 4 in acrosome formation during spermiogenesis of rats. Eur J Biochem 2001; 268:3053–3061.
60. O'Flaherty C, de Souza AR. Hydrogen peroxide modifies human sperm peroxiredoxins in a dose-dependent manner. Biol Reprod 2011; 84: 238–247.
61. Iuchi Y, Okada F, Tsunoda S, Kibe N, Shirasawa N, Ikawa M, Okabe M, Ikeda Y, Fujii J. Peroxiredoxin 4 knockout results in elevated spermatogenic cell death via oxidative stress. Biochem J 2009; 419: 149–158.
62. Guo Z, Deshpande R, Paull TT. ATM activation in the presence of oxidative stress. Cell Cycle 2010; 9:4805–4811.
63. Murphy MP. Nitric oxide and cell death. Biochim Biophys Acta 1999; 1411:401–414.
64. Vasko MR, Guo C, Thompson EL, Kelley MR. The repair function of the multifunctional DNA repair/redox protein APE1 is neuroprotective after ionizing radiation. DNA Repair (Amst) 2011; 10:942–952.